Coordinative Behavior of the CNCN Ligand. Experimental and Density Functional Study of Spectroscopic Properties and Bonding in the $Cr(CO)_5CNCN$ Complex

Maxim P. Aarnts and Derk J. Stufkens*

Anorganisch Chemisch Laboratorium, J. H. van't Hoff Research Institute, Nieuwe Achtergracht 166, 1018 WV Amsterdam, The Netherlands

Miquel Solà† and Evert Jan Baerends*

Scheikunding Laboratorium der Vrije Universiteit, De Boelelaan 1083, 1081 HV Amsterdam, The Netherlands

Received October 31, 1996⊗

The coordinative behavior of the CNCN ligand is investigated experimentally, by means of UV−Vis, UV-photoelectron, and IR spectra of the $Cr(CO)_5CNCN$ complex and, theoretically, by means of density functional calculations on the same complex and on the free CNCN ligand. The density functional calculations give accurate results for the spectroscopic properties of these compounds. Special attention is paid to a comparison of the CO and CNCN ligands. First bond dissociation energies, and various components of this bond obtained by an energy decomposition, are compared for L = CO and L = CNCN in the $Cr(CO)_5L$ complexes. It is found that the σ-base properties of CO and CNCN are quite similar, while CNCN is found to be an only slightly stronger π acid than CO in spite of a much lower lying π^* LUMO. The π-acceptor capability of CNCN is not much larger than that of CO because the CNCN $3\pi^*$ has lower amplitude than the CO $2\pi^*$ at the coordinating C, leading to smaller overlap with the π-donor orbital of the metal fragment.

Introduction

The synergetic bonding mechanism of π-acid ligands when attached to transition metal atoms in low-positive, zero, or negative formal oxidation states has been recognized for a long time and has been used to explain the electronic structure of π complexes.[1] These π-acid ligands have, in addition to σ lone pairs by which they can form the usual donative coordinative bond, low-lying vacant π orbitals that can act as acceptor orbitals in the π backdonation. Among the π-acid ligands the most well-known is carbon monoxide, but also N_2, CS, NO, isocyanides, and substituted phosphines, arsines, stibines, or sulfides are examples of this kind of ligand.

In 1988, Van der Does and Bickelhaupt[2] synthesized the isocyanogen, CNCN, a new π-acid ligand of the group of the isocyanides, by pyrolyzing norbornadienone azine. Yamada *et al.*[3a] were also able to obtain CNCN as a pyrolysis product of *n*-cyano-2,3-diphenylcyclopropeneimine, while Blanch and McCluskey[3b] synthesized it by ambient light photolysis of gaseous BrCN, ClCN, and ICN. Although originally reported as CNNC, CNCN was unambiguously identified by Stroh and Winnewiser[4] in the gas phase on the basis of its high-resolution Fourier transform infrared (FTIR) and microwave spectra. Later infrared spectra (IR),[5] ultraviolet photoelectron (UV−PES) spectra,[6] microwave,[7] and ^{13}C and ^{15}N NMR spectral studies,[8] as well as a number of theoretical investigations,[9] have confirmed the CNCN molecule to be the main product of these pyrolyses. The mechanisms of these reactions have been discussed[10,11] and the CNCN molecule was proposed to be formed by isomerization of CNNC.

† Permanent address: Institut de Química Computacional and Departament de Química, Universitat de Girona, 17071 Girona, Catalonia, Spain.

⊗ Abstract published in *Advance ACS Abstracts,* April 1, 1997.

(1) (a) Cotton, F. A.; Wilkinson, G. *Advanced Inorganic Chemistry*, 5th, Ed.; John Wiley & Sons: New York, 1988. (b) Nakamoto, K. *Infrared and Raman Spectra of Inorganic and Coordination Compounds*, 3rd, ed.; John Wiley & Sons: New York, 1978.

(2) Van der Does, T.; Bickelhaupt, F. *Angew. Chem.* **1988**, *100*, 998.

(3) (a) Yamada, K. M. T.; Markus, M. W.; Winnewiser, G.; Joentgen, W.; Kock, R.; Vogel, E.; Altenbach, H.-J. *Chem. Phys. Lett.* **1989**, *160*, 113. (b) Blanch, R. J.; McCluskey, A. *Chem. Phys. Lett.* **1995**, *241*, 116.

(4) (a) Stroh, F.; Winnewiser, M. *Chem. Phys. Lett.* **1989**, *155*, 21. (b) Seibert, J. W. G.; Winnewiser, M.; Winnewieser, B. P.; Bickelhaupt, F. *J. Mol. Struct.* **1996**, *376*, 229. (c) Stroh, F.; Winnewieser, M.; Winnewieser, B. P. *Can. J. Phys.* **1994**, *72*, 1251.

(5) Stroh, F.; Winnewiser, B. P.; Winnewiser, M.; Reisenauer, H. P.; Maier, G.; Goede, S. J.; Bickelhaupt, F. *Chem. Phys. Lett.* **1989**, *160*, 105.

(6) (a) Grabandt, O.; De Lange, C. A.; Mooyman, R.; Van der Does, T.; Bickelhaupt, F. *Chem. Phys. Lett.* **1989**, *155*, 221. (b) Cederbaum, L. S.; Tarantelli, F.; Weikert, H.-G.; Scheller, M.; Köppel, H. *Angew. Chem.* **1989**, *101*, 770. (c) Scheller, M. K.; Weikert, H. G.; Cederbaum, L. S.; Tarantelli, F. *J. Electron Spectrosc.* **1990**, *51*, 75.

(7) Gerry, M. C. L.; Stroh, F.; Winnewiser, M. *J. Mol. Spectrosc.* **1990**, *140*, 147.

(8) Goede, S. J.; de Kanter, F. J. J.; Bickelhaupt, F. *J. Am. Chem. Soc.* **1991**, *113*, 6104.

(9) (a) Bickelhaupt, F. M.; Nibbering, N. M. M.; van Wezenbeek, E. M.; Baerends, E. J. *J. Phys. Chem.* **1992**, *96*, 4864. (b) Von Niessen, W.; Cederbaum, L. S.; Schirmer, J.; Diercksen, G. H. F.; Kraemer, W. P. *J. Electron Spectrosc.* **1982**, *28*, 45. (c) Scheller, M. K.; Weikert, H. G.; Cederbaum, L. S.; Tarantelli, F. *J. Electron Spectrosc.* **1990**, *51*, 75. (d) De Almeida, W. B.; Hinchliffe, A. *J. Mol. Struct. (THEOCHEM)* **1990**, *206*, 77. (e) Sana, M.; Leroy, G. *J. Mol. Struct.* **1981**, *76*, 259. (f) Haese, N. H.; Woods, R. C. *J. Chem. Phys.* **1980**, *73*, 4521. (g) Botschwina, P.; Sebald, P. *Chem. Phys.* **1990**, *141*, 311. (h) Nguyen, M. T. *Chem. Phys. Lett.* **1989**, *157*, 430. (i) Sherrill, C. D.; Schaefer, H. F. *J. Chem. Phys.* **1994**, *100*, 8920.

(10) Goede, S. J.; de Kanter, F. J. J.; Bickelhaupt, F. *J. Am. Chem. Soc.* **1991**, *113*, 6104.

(11) Sunil, K. K.; Yates, J. K.; Jordan, K. D. *Chem. Phys. Lett.* **1990**, *171*, 185.

S0276-7333(96)00921-1 CCC: $14.00

Although the synthesis of CNCN is quite recent, the first complex containing isocyanogen was reported in 1982.[12] It was the $Cr(CO)_5CNCN$ complex, synthesized by reaction of $NEt_4[Cr(CN)(CO)_5]$ with cyanogen chloride. In this work, the most intense IR bands of this complex were also reported. In a more recent study, the IR and Raman spectra of this complex were determined and interpreted.[13] The authors concluded that the bonding properties remain practically unchanged when going from $Cr(CO)_6$ to $Cr(CO)_5CNCN$ because of their very similar vibrational spectra and the absence of a dipole moment also in the latter case. These observations contradicted the earlier suggestion by other authors[12] that CNCN is a much better π-acceptor ligand than CO.

This paper reports the experimental and calculated (density functional (DF)) UV−PES and UV−vis absorption spectra of the $Cr(CO)_5CNCN$ complex. Also a comparison of the theoretical IR spectrum and the previously reported experimental[12,13] one is performed. Since there is a large number of experimental[14] and theoretical[15] studies on the octahedral $Cr(CO)_6$ complex, this hexacarbonyl compound will be taken as a reference in order to compare the changes undergone by the complex when a CO is substituted by a CNCN. Actually, given that a comparison between the CNCN and CO ligands has not yet been performed, one of the main goals of this work is to analyze the differences between both ligands. To this end, DF calculations are performed for the bond energies of both ligands to the $Cr(CO)_5$ metal fragment and various components of the bond—steric repulsion, σ bonding, and π backbonding—are obtained.

Experimental Section

Preparation. The $Cr(CO)_5(CNCN)$ complex was synthesized according to a literature procedure[13] by reaction of CNCN with $Cr(CO)_5$(2-MeTHF) at −40 °C. This latter complex was obtained by irradiation of $Cr(CO)_6$ in 2-MeTHF at room temperature. $Cr(CO)_5(CNCN)$ was isolated in moderate yield. After column chromatography over activated silica gel (Kieselgel 60, Merck, 70-238 mesh) with pentane as eluent, the compound had a purity of more than 97%.

Spectroscopic Measurements and Instrumentation. The He I photoelectron spectrum was recorded on a Perkin-Elmer PS-18 photoelectron spectrometer with a Helectros Developments hollow cathode He I/He II light source. The spectrum was calibrated with respect to He, Ar, and Xe lines as internal references. The sample temperature was kept at 25 °C, in order to get a slow, continuous evaporation into the reaction chamber. IR spectra were measured on a BioRad FTS-A60 FTIR spectrometer equipped with a liquid nitrogen cooled MCT detector. Electronic absorption spectra were recorded on a Varian Cary 4E spectrometer. Low-temperature UV−vis and IR measurements were carried out using an Oxford Instruments DN 1704/54 liquid nitrogen cryostat. The light source for the photochemical experiments was an Oriel high-pressure Hg lamp, equipped with a 313 nm interference filter.

Computational Details. All calculations were performed with the Amsterdam Density Functional (ADF) program system.[16] An uncontracted triple-ζ STO basis set[17] was used for chromium (cf. basis set IVA in ref 15i). The ligand atoms were represented by a double-ζ STO basis set[17] extended with one 3d polarization function. The 1s electrons on C, N, and O as well as the 1s, 2s, and 2p electrons on Cr were considered as core electrons and treated by the frozen-core approximation.[16a] As shown before for the CO molecule,[18] and for the $Cr(CO)_5$−CO bond,[15i] this basis set is adequate to describe spectroscopic properties with reasonable accuracy. In order to fit the molecular density and to present Coulomb and exchange potentials accurately, a set of auxiliary s, p, d, f, and g STO functions, centered on all nuclei, was introduced.[19,15i]

Geometries were fully optimized within the C_{4v} symmetry group, with the local density approximation (LDA), which includes the Xα exchange[20] ($\alpha = {}^2/_3$), together with the electron gas correlation functional (in the Vosko−Wilk−Nusair parametrization[21]), where according to Stoll *et al.*[22] only the correlation between electrons of different spin is used. The optimization of the $Cr(CO)_5CNCN$ complex has also been performed including nonlocal (LDA-NL) corrections in order to compare the LDA and LDA-NL optimized geometries. The molecular geometries were optimized using the analytical energy gradients implemented by Versluis and Ziegler[23] at the LDA level and by Fan and Ziegler[24] at the LDA-NL level. Harmonic frequencies were calculated by two-point numerical differentiation using Cartesian displacements of $\pm 0.05 a_o$.

Energies were evaluated within the LDA approach and also including nonlocal corrections. At the LDA-NL level, exchange was described with Slater's[20] $\rho^{4/3}$ approximation (Xα, with $\alpha = {}^2/_3$), with a nonlocal correction of Becke,[25] and with the nonlocal correlation correction due to Perdew.[26] In the computation of the UV−vis spectra, the multiplet energies were calculated in the way suggested by Ziegler *et al.*[27] Only vertical transitions were considered.

In the analysis of the bonding mechanism, the total energy difference is decomposed into the deformation energy (ΔE_{def}) needed to bring the fragments to the geometry that they have

(12) Christian, G.; Stolzenberg, H.; Fehlhammer, W. P. *J. Chem. Soc., Chem. Commun.* **1982**, 184.

(13) Schoemaker, G. C.; Stufkens, D. J.; Goede, S. J.; van der Does, T.; Bickelhaupt, F. *J. Organomet. Chem.* **1990**, *390*, C1.

(14) (a) Lewis, K. E.; Golden, D. M.; Smith, G. P. *J. Am. Chem. Soc.* **1984**, *106*, 3905. (b) Rees, B.; Mitschler, A. *J. Am. Chem. Soc.* **1976**, *98*, 7918. (c) Loubriel, G.; Plummer, E. W. *Chem. Phys. Lett.* **1979**, *64*, 234. (d) Plummer, E. W.; Salaneck, W. R.; Miller, J. S. *Phys. Rev. B* **1978**, *18*, 1673. (e) Hargittai, M.; Hargittai, I. *The Molecular Geometries of Coordination Compounds in the Vapour Phase*; Elsevier: New York, 1977; p 187. (f) Beach, N. A.; Gray, H. B. *J. Am. Chem. Soc.* **1968**, *90*, 5713.

(15) (a) Baerends, E. J.; Rozendaal, A. In *Quantum Chemistry: The Challenge of Transition Metal and Coordination Chemistry*; Veillard, A., Ed.; Kluwer: Dordrecht, The Netherlands, 1986; p 159. (b) Arratia-Perez, R.; Yang, C. Y. *J. Chem. Phys.* **1985**, *83*, 4005. (c) Barnes, L. A.; Rosi, M.; Bauschlicher, C. W., Jr. *J. Chem. Phys.* **1991**, *94*, 2031. (d) Barnes, L. A.; Liu, B.; Lindh, R. *J. Chem. Phys.* **1993**, *98*, 3978. (e) Li, J.; Schreckenbach, G.; Ziegler, T. *J. Phys. Chem.* **1994**, *98*, 4838. (f) Ehlers, A. W.; Dapprich, S.; Vyborshchikov, S. F.; Frenking, G. *Organometallics* **1996**, *15*, 105. (g) Schreckenbach, G.; Ziegler, T.; Li, J. *Int. J. Quantum Chem.* **1995**, *56*, 477. (h) Ehlers, A. W., Frenking, G. *J. Am. Chem. Soc.* **1994**, *116*, 1514. (i) Rosa, A.; Ehlers, A. W.; Baerends, E. J.; Snijders, J. G.; te Velde, G. *J. Phys. Chem.* **1996**, *100*, 5690.

(16) (a) Baerends, E. J.; Ellis, D. E.; Ros, P. *Chem. Phys.* **1973**, *2*, 41. (b) Boerrigter, P. M.; te Velde, G.; Baerends, E. J. *Int. J. Quant. Chem.* **1988**, *33*, 87. (c) te Velde, G.; Baerends, E. J. *J. Comput. Phys.* **1992**, *99*, 84.

(17) (a) Snjiders, J. G.; Baerends, E. J.; Vernooijs, P. *At. Nucl. Data Tables* **1982**, *26*, 483. (b) Vernooijs, P.; Snijders, J. G.; Baerends, E. J. Slater type basis functions for the whole periodic system. Internal report; Free University of Amsterdam, The Netherlands, 1981.

(18) Baerends, E. J; Vernooijs, P.; Rozendaal, A.; Boerrigter, P. M.; Krijn, M.; Feil, D.; Sundholm, D. *J. Mol. Struct. (THEOCHEM)* **1985**, *133*, 147.

(19) Krijn, J.; Baerends, E. J. Fit functions in the HFS-method. Internal report; Free University of Amsterdam, The Netherlands, 1984.

(20) Slater, J. C. *Quantum Theory of Molecules and Solids;* McGraw-Hill: New York, 1974; Vol. 4.

(21) Vosko, S. H.; Wilk, L.; Nusair, M. *Can. J. Phys.* **1980**, *58*, 1200.

(22) Stoll, H.; Golka, E.; Preuss, H. *Theor. Chim. Acta* **1980**, *55*, 29.

(23) Versluis, L.; Ziegler, T. *J. Chem. Phys.* **1988**, *28*, 322.

(24) Fan, L.; Ziegler, T. *J. Chem. Phys.* **1991**, *95*, 7401.

(25) (a) Becke, A. D. *J. Chem. Phys.* **1986**, *84*, 4524. (b) Becke, A. D. *Phys. Rev. A* **1988**, *38*, 3098. (c) Becke, A. D. *Int. J. Quantum Chem.* **1983**, *23*, 1915.

(26) Perdew, J. P. *Phys. Rev. B* **1986**, *33*, 8822.

(27) Ziegler, T.; Rauk, A.; Baerends, E. J. *Theor. Chim. Acta* **1977**, *43*, 261.

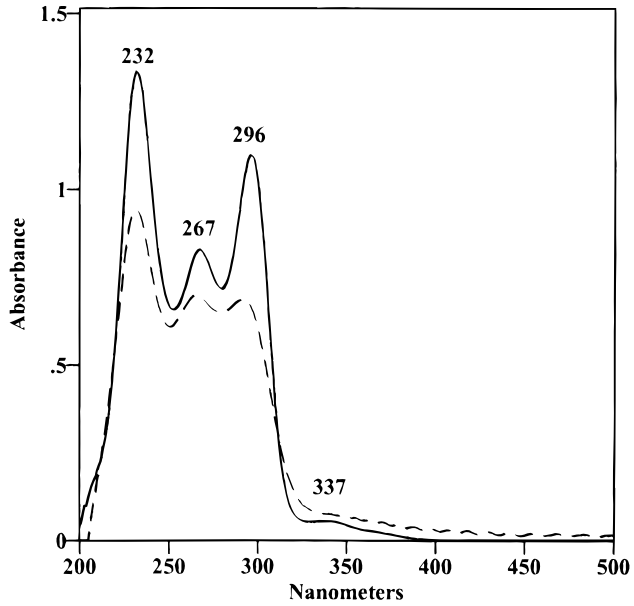

Figure 1. Experimental UV−vis spectrum of the Cr(CO)$_5$CNCN complex in dimethylbutane/pentane (8:3) at room temperature (---) and 77 K (—).

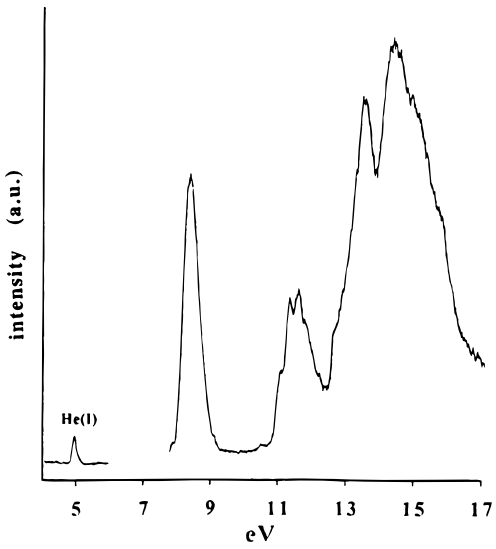

Figure 2. Experimental He I photoelectron spectrum of the Cr(CO)$_5$CNCN complex.

in the complex and the interaction energy (ΔE_{int}). This interaction energy is explicitly split up in the steric repulsion (ΔE^0) and orbital interaction (ΔE_{oi}) parts.[28] The steric repulsion between two interacting systems A and B is the energy difference between the wave function

$$\Psi^0 = NA[\Psi_A\Psi_B]$$

and the isolated systems A and B. Ψ^0 is the normalized (operator N) and antisymmetrized (operator A) product of the monomer wave functions. It comprises both the classical electrostatic interaction (ΔE_{elstat}) between the unperturbed charge distributions of the fragments and (in an orbital method like Kohn−Sham) the four-electron destabilizing interactions between occupied orbitals (Pauli repulsion, ΔE_{Pauli}). The orbital interaction, ΔE_{oi}, accounts for charge transfer (interaction between occupied orbitals in one moiety with unoccupied orbitals of the other, including the HOMO−LUMO interactions) and polarization (empty/occupied orbital mixing on one fragment). The ΔE_{oi} has, however, not been decomposed into these terms but it has been decomposed, according to the extended transition-state method (ETS),[28b,c] into contributions from the different irreducible representations in which the orbital interactions occur. This means that in the pertinent C_{4v} symmetry the A_1 energy component is associated with the σ component of the bond between Cr(CO)$_5$ and CNCN, while the E component reflects the strength of the π (back)bonding.

Results and Discussion

1. Experimental Spectra. The UV−vis absorption spectrum of the complex was recorded in dimethylbutane/pentane (8:3) both as a solution at room temperature and as a glass at 77 K (Figure 1). The four absorptions do not shift but only show a change of relative intensities at lower temperature. The absorption maxima are collected in Table 6 together with the assignments, which will be discussed in a later section.

The UV−PES spectrum of Cr(CO)$_5$(CNCN), obtained by He I excitation, is presented in Figure 2. The ionization energies derived from this spectrum are collected in Table 7 together with the theoretical data. The assignments and correlations between experiment and theory will be discussed hereafter.

In a previous article on the IR and Raman spectra of the complex,[13] a band at 1950 cm^{-1} was tentatively assigned to a different complex, possibly the isomer Cr(CO)$_5$(NCNC). In order to find out whether we are dealing here with an equilibrium between these two complexes, IR spectra were recorded in 2-MeTHF in the temperature range 170−290 K and in pentane between 190 and 290 K. These experiments did not give evidence for such an equilibrium since the intensity of the 1950 cm^{-1} band did not change with respect to those of the bands assigned to Cr(CO)$_5$(CNCN).

2. Theoretical Results. In this section we present the results of the calculations, starting with the geometries and IR spectra of the CO and CNCN ligands. Next, the geometry of the Cr(CO)$_5$CNCN complex is analyzed followed by the first bond dissociation energies of the two ligands for which an energy decomposition is performed. Finally the UV−vis, UV−PES, and IR spectra of Cr(CO)$_5$CNCN are calculated and the results are compared with the experimental data.

(a) Preliminary Study of the Ligands. The purpose of this section is twofold. The first goal is to collect the geometry and the IR spectra of the free CO and CNCN ligands as a reference for studying the changes undergone by these ligands in the Cr(CO)$_5$CNCN complex. We will also compare the density functional results with previously reported *ab initio* calculations for the free ligands.

Tables 1 and 2 report the geometry, dipole moment, and harmonic frequencies of CO and CNCN molecules, respectively. Experimental frequencies for the CNCN molecule in Table 2 are the observed frequencies which contain nonharmonic contributions.

It has been already noted[29−31] that in DFT calculations of organic molecules the single bonds between non-

(28) (a) Kitaura, K; Morokuma, K. *Int. J. Quantum Chem.* **1976**, *10*, 325. (b) Ziegler, T.; Rauk, A. *Theor. Chim. Acta* **1977**, *46*, 1. (c) Ziegler, T.; Rauk, A. *Inorg. Chem.* **1979**, *18*, 1755.

(29) Johnson, B. G.; Gill, P. M. W.; Pople, J. A. *J. Chem. Phys.* **1993**, *98*, 5612.

(30) (a) Andzelm, J.; Wimmer, E. *Physica B* **1991**, *172*, 307. (b) Andzelm, J.; Wimmer, E. *J. Chem. Phys.* **1992**, *96*, 1280.

(31) Murray, C. W.; Laming, G. J.; Handy, N. C.; Amos, R. D. *Chem. Phys. Lett.* **1992**, *199*, 551.

Table 1. Bond Length (R_{C-O} in Å), Dipole Moment (μ in D), and Harmonic Frequency (ν_e in cm^{-1}) for the CO Molecule[a]

	R_{C-O}	μ	ν_e
LDA	1.136	−0.150	2151.6
LDA-NL	1.136	−0.089	2137.2
6-31G*[b]	1.114	+0.264	2439
MP2/6-31G*[b]	1.150	−0.192	2125
QCISD/6-31G*[b]	1.145	+0.011	2176
QCISD/6-311++G**[c]	1.134	−0.082	
exp[d]	1.128	−0.122	2170.2[e]

[a] A negative dipole means the positive end of the dipole is toward oxygen. [b] From ref 29. [c] From ref 38. [d] From ref 18. [e] The fundamental frequency is 2143 cm^{-1} (ref 1b).

hydrogen atoms are too short by 0.01−0.02 Å, while triple bonds are too long by ∼0.01 Å. This trend is also observed in the CO and CNCN systems for both the LDA and LDA-NL approaches. The CN−CN single bond length is found 0.019 Å shorter and the CO and CN triple bonds are found 0.008−0.013 Å longer than the experimental values. Nevertheless, the bond length accuracy obtained with the DFT approach is comparable to, actually slightly better than, that obtained with second-order Møller−Plesset perturbation theory (MP2).

As previously shown for the CO and NO molecule,[29] DFT is successful in computing the sign of dipole moments with values close to zero. On the other hand, it is well-known that CO is predicted to have the wrong sign in Hartree−Fock (HF) calculations. Interestingly, the values obtained for the dipole moments of the CO and CNCN molecules using the DFT approach are the most precise among the different methodologies compared.

For vibrational frequencies, the HF results are well-known to be systematically large by ∼10−15%. Again, DFT calculations at LDA and LDA-NL levels show the characteristics of a correlated electronic structure, and their predicted frequencies are closer to the experimental ones than MP2 frequencies. In fact, only CEPA calculations are found to be in slightly better agreement with experiment. Interestingly, LDA and LDA-NL harmonic frequencies are very similar, i.e., nonlocal corrections have a rather modest influence in calculated frequencies, their main effect being to decrease the frequencies by ∼10−15 cm^{-1}. A similar result was reported by Bérces and Ziegler,[32] who found that differences between LDA and LDA-NL harmonic frequencies are mainly related to the differences in optimized geometries. If we restrict ourselves to the LDA results, which will be used for the complex, we observe that for CO the calculated harmonic frequency of 2152 cm^{-1} is somewhat higher (∼10 cm^{-1}) than the measured fundamental at 2143 cm^{-1}. The anharmonicity correction being close to +30 cm^{-1}, the calculated harmonic frequency is still some 20 cm^{-1} lower than the experimental ν_e. For the high-frequency modes of CNCN, ν_1 and ν_2, we find that the calculated harmonic ones are also higher than the measured fundamentals (some 20 cm^{-1}), but if the anharmonicity correction for the CNCN triple bonds is similar to that for the CO triple bond, the calculated harmonic frequencies are probably still a bit too low. The largest disagreement between theoretical and experimental frequencies is found for the ν_3 and ν_4 frequencies. This is likely to be the result of a Fermi resonance between ν_3 and $2\nu_4$, as pointed out by Botschwina and Sebald.[9g] This interaction would increase the observed ν_3 frequency and decrease ν_4. On the whole, one can conclude that the DFT/DZP scheme seems quite appropriate to undertake a study of the $Cr(CO)_5CNCN$ spectroscopic properties at reasonable computing cost.

(b) Geometry of the $Cr(CO)_5CNCN$ Complex. The LDA, LDA-NL, and experimental geometries of the $Cr(CO)_5CNCN$ complex are reported in Table 3. The geometry parameters used in this table are described in Figure 3. The dipole moment for this complex is found to be 2.377 and 2.470 D at the LDA and LDA-NL levels, respectively.

The values of Table 3 show that LDA metal−ligand bond lengths are shorter than experimental by 0.02−0.03 Å. Inclusion of nonlocal corrections tends to elongate these bonds[33] and improves the agreement between theory and experiment. At the LDA-NL level, the remaining differences between calculated and experimental metal−ligand bond lengths range from 0.01 ($Cr-CO_{ax}$ and Cr−CNCN) to 0.03 Å ($Cr-CO_{eq}$). (The mean square deviations of calculated bond lengths from the experimental ones are 0.029Å for LDA and 0.026Å for NLDA, respectively.)

Here too we find that the CN and CO calculated triple bonds are too long, by 0.02−0.04 Å, i.e., slightly more so than in the free ligands. As expected,[1] the back-bonding mechanism of π complexes leads to a lengthening of the calculated CO and CN triple bonds as compared to those found in the CO and CNCN free ligands. Surprisingly, this is not reproduced by the experimental data either for CNCN or for CO. For instance, the experimental C−NCN and CNC−N bond lengths in the CNCN molecule are 1.175 and 1.158 Å, whereas in the complex they are found to be 1.167 and 1.132 Å.[12] Also, the C−O bond length in the CO free molecule is 1.128 Å and is reported to be 1.125 Å for the $C-O_{ax}$ in the $Cr(CO)_5CNCN$ complex. More often a slight contraction of the triple CO bond in carbonyl complexes is observed, in contrast to the expected bond weakening and lengthening. The latter is always calculated and fits in with the generally observed IR frequency lowering of the CO stretch vibration. We have not been able to find an explanation for this discrepancy.

The optimized Cr−C and C−O bond lengths for the $Cr(CO)_6$ complex with the basis set used in this study are 1.869 and 1.151 Å at the LDA level and 1.910 and 1.152 Å when nonlocal corrections are added to the exchange-correlation functional. When these Cr−C and C−O bond lengths in the $Cr(CO)_6$ complex are compared to those of the $Cr(CO)_5CNCN$ system, it is found that substitution of a CO by a CNCN molecule in the $Cr(CO)_6$ complex has virtually no effect on the C−O bond distance and slightly increases the Cr−C bond length by ∼0.01 Å.

The theoretically derived lengthening of the C−NCN and CNC−N triple bonds and the shortening of the CN−CN single bond in the complex, as compared to the free CNCN molecule, can be understood by taking into account the shape of the LUMO orbital of the CNCN ligand and the effects of the π-backbonding mechanism. The LUMO orbital of CNCN is a $3\pi^*$ orbital which has

(32) Bérces, A.; Ziegler, T. *J. Phys. Chem.* **1995**, *99*, 11417.

(33) Ziegler, T. *Chem. Rev.* **1991**, *91*, 651.

Table 2. Bond Lengths (Å), Dipole Moment (D), and Theoretical Harmonic Frequencies (cm^{-1}) and Experimental Fundamental Frequencies for the CNCN Molecule

	R_{C-NCN}	R_{CN-CN}	R_{CNC-N}	μ	ν_1	ν_2	ν_3	ν_4	ν_5
LDA	1.188	1.297	1.169	−0.701	2320.9	2081.8	957.2	501.6	230.2
LDA-NL	1.188	1.298	1.166	−0.795	2311.7	2073.2	949.4	485.8	214.4
MP2[a]	1.191	1.318	1.176		2287	2036	926	455	190
MP2[b]	1.216	1.341	1.214	−0.166	2191	1903	859	508	243
CISD[b]	1.195	1.329	1.177	−0.837					
CISD[c]	1.166	1.316	1.142		2505	2229	969	508	201
CEPA[d]	1.181	1.322	1.158	−0.704	2318.9	2073.4	912.5	477	194
exp	1.175[e]	1.316[e]	1.158[e]	−0.707[e]	2302.0[f]	2059.7[f]	975[f]	463.5[f]	197.8[f]

[a] MP2/6-31G* from ref 9h. [b] MP2/D95 and CISD/D95 from ref 9d. [c] CISD/TZ2P from ref 9i. [d] CEPA/104 CGTOs from ref 9g. [e] Reference 7. [f] Reference 5.

Table 3. LDA, LDA-NL, and Experimental Geometry of the $Cr(CO)_5CNCN$ Complex[a]

	$R_{Cr-COax}$	$R_{Cr-COeq}$	$R_{Cr-CNCN}$	R_{C-Oax}	R_{C-Oeq}	R_{C-NCN}	R_{CN-CN}	R_{CNC-N}	ϕ
LDA	1.874	1.884	1.863	1.150	1.150	1.195	1.285	1.173	90.4
LDA-NL	1.923	1.932	1.890	1.151	1.152	1.195	1.286	1.172	90.6
exp[a]	1.913	1.903	1.883	1.125	1.128	1.167	1.280	1.132	

[a] Geometry parameters are specified in Figure 3. Bond lengths are given in angstroms and the angle in degrees. [b] From ref 12.

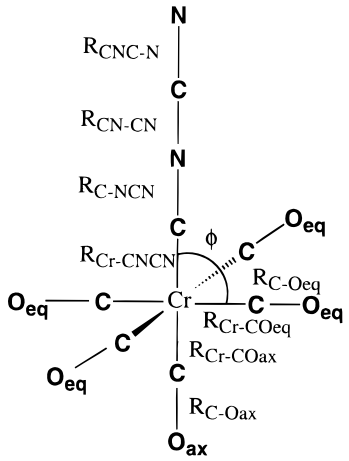

Figure 3. Optimized geometrical parameters in the C_{4v} structure of the $Cr(CO)_5CNCN$ complex.

antibonding character in the triple bonds and bonding character in the single bond. Therefore, any supply of charge from the 3d orbitals of Cr to the $3\pi^*$ orbital of the CNCN molecule is expected to result in larger CN triple bond lengths and a shorter CN−CN single bond distance, as indeed found in the calculations. Experimentally there appears to be an overall shortening of all ligand bonds of 0.02−0.03 Å compared to the calculations, yielding an extremely short CN−CN single bond and slightly shortened rather than lengthened triple bonds.

Here a last remark must be made. In the experimental work,[12] it was found that the CNCN moiety bends considerably (CNC angle, 168.5°). Further geometry optimization of the $Cr(CO)_5CNCN$ complex without symmetry constraints has not lead to an appreciable distortion of the CNCN linearity. Moreover, we do not see any electronic reason for the CNCN bending. We have calculated the energy of a structure with a CNC angle of 165.5°, which is only 0.41 kcal/mol above the linear structure. Therefore, we have concluded that a crystal effect can be responsible for the observed considerable deviation from linearity of the CNCN moiety in the $Cr(CO)_5CNCN$ complex.

(c) Energetics and Fragment Analysis. The main objective of this section is to compare the first bond dissociation energy (FBDE) of the CNCN ligand in the $Cr(CO)_5CNCN$ complex, and its components, to those of CO in the $Cr(CO)_6$ complex. The latter has also been determined experimentally.[14a] All FBDEs were decomposed into their components according to the ETS method.[28] The results are collected in Tables 4 and 5. Thermal corrections and contributions to the vibrational zero-point energy correction are not included but are expected to be small on the basis of previous studies.[15c−e] Deformation energies from free fragments to the structures of the fragments in the complex were computed from the energy of the geometry-optimized structures of the fragments. Optimization of the $Cr(CO)_5$ fragment has been performed keeping the C_{4v} symmetry of a square pyramidal structure, since previous experimental[34] studies have shown that $Cr(CO)_5$ possesses C_{4v} symmetry. Furthermore, it was theoretically reported[35] that the D_{3h} structure of a trigonal bipyramid for

Table 4. Overlaps between Frontier Orbitals, Mulliken Populations of the Frontier Orbitals, and Contributions to the Bond Energy (eV) between the $Cr(CO)_5$ and CO Fragments

	LDA	LDA-NL
	Overlaps	
(5σ, $10a_1$)	0.462	0.437
($2\pi^*$, 8e)	0.177	0.170
	Populations	
$10a_1$	0.365	0.316
8e	1.824	1.829
5σ,	1.557	1.621
$2\pi^*$	0.204	0.200
	Energies	
ΔE_{Pauli}	5.051	4.648
ΔE_{elstat}	−3.895	−3.302
ΔE^o	1.156	1.346
ΔE_{oi}	−3.698	−3.264
A_1	−1.899	−1.620
E	−1.772	−1.640
A_2,B_1,B_2	−0.010	−0.006
ΔE_{rest}[a]	−0.017	0.002
ΔE_{int}	−2.542	−1.918
ΔE_{def}	0.075	0.089
ΔE_{total}	−2.467	−1.829

[a] Error due to the use of the fitted density instead of exact one in energy decomposition.

(34) (a) Graham, M. A.; Poliakoff, M.; Turner, J. J. *J. Chem. Soc. A* **1977**, 2939. (b) Perutz, R. N.; Turner, J. J. *Inorg. Chem.* **1975**, *14*, 262. (c) Perutz, R. N.; Turner, J. J. *J. Am. Chem. Soc.* **1975**, *97*, 4791. (d) Perutz, R. N.; Turner, J. J. *J. Am. Chem. Soc.* **1975**, *97*, 4800..

Table 5. Overlaps between Frontier Orbitals, Mulliken Populations of the Frontier Orbitals, and Contributions to the Bond Energy (eV) between the $Cr(CO)_5$ and CNCN Fragments

	LDA	LDA-NL
	Overlaps	
(9σ, $10a_1$)	0.462	0.440
($3\pi^*$, 8e)	0.141	0.138
	Populations	
$10a_1$	0.371	0.323
8e	1.776	1.776
9σ	1.558	1.629
$3\pi^*$	0.225	0.223
	Energies	
ΔE_{Pauli}	5.371	5.129
ΔE_{elstat}	−4.261	−3.708
ΔE^o	1.110	1.421
ΔE_{oi}	−4.030	−3.698
A_1	−1.973	−1.734
E	−2.043	−1.974
A_2, B_1, B_2	−0.010	−0.005
ΔE_{rest}[a]	−0.004	0.015
ΔE_{int}	−2.920	−2.277
ΔE_{def}	0.072	0.127
ΔE_{total}	−2.848	−2.150

[a] Error due to the use of the fitted density instead of exact one in energy decomposition.

$Cr(CO)_5$ was ∼9 kcal/mol higher in energy than the square pyramidal structure for the same complex.

In order to gain more insight into the nature of the nonlocal corrections, we have calculated the energy contributions to the FBDEs at the LDA and LDA-NL levels. Most trends when going from LDA to LDA-NL are the same for the CO (Table 4) and CNCN (Table 5) ligands. When nonlocal corrections are included in the exchange-correlation functional, we have found, for the two cases, a decrease in the Pauli repulsion term and a quantitatively more important reduction of the electrostatic interaction. As a result, the LDA-NL total steric repulsion energies ΔE^0 become larger than the LDA ones. The effect of the nonlocal corrections is rather intricate, since both the Pauli repulsion and the electrostatic attraction are quite sensitive to the bond length, and the observed changes from LDA to LDA-NL are primarily caused by the larger Cr−L bond length at the LDA-NL level. Similarly, the LDA-NL orbital interaction energy is smaller than the LDA one, mostly due to smaller overlaps due to larger bond lengths. As a whole, the final LDA-NL interaction energies are smaller than the LDA ones.

Table 4 gives the components of the FBDE for the $Cr(CO)_5$ + CO fragments in the $Cr(CO)_6$ O_h complex at the LDA and LDA-NL levels. The experimental gas-phase FBDE obtained using pulsed laser pyrolysis techniques is −36.8 ± 2 kcal/mol.[14a] Our calculated FBDEs are −56.9 and −42.2 kcal/mol at the LDA and LDA-NL levels of theory, respectively. As expected, the LDA approach overestimates the binding energy by ∼20 kcal/mol. The best estimate computed at the LDA-NL level with a more extended basis set and including corrections for the basis set superposition error (BSSE) yields −41.5 kcal/mol,[15i] slightly too high as compared to the experimental value but quite close to the value found here. Interestingly, the A_1 and E contributions to the orbital interaction energy are very similar. The stabilizing ΔE_E reflects the π backbonding, but in A_1 symmetry there are, apart from the σ donation, considerable polarization effects, presumably due to the large amplitude of the 5σ orbital toward the metal fragment, which induces electrostatic polarization effects.

The results gathered in Tables 4 and 5 allow a comparison to be made between the CO and the CNCN ligands. As a preliminary, it is worth noting that at the LDA level the HOMO (5σ) and LUMO ($2\pi^*$) energies of the CO molecule are −8.725 and −1.809 eV, respectively. For the CNCN, the HOMO (9σ) and LUMO ($3\pi^*$) have energies of −8.616 and −3.395 eV. Therefore, from the energy values of the HOMO and LUMO of CO and CNCN, one can expect that the CNCN molecule is likely to have a similar σ-base character but a much better π-acceptor character than CO, as previously suggested.[12]

The CNCN is indeed found to have a larger FBDE to the $Cr(CO)_5$ fragment than the CO ligand, both at the LDA and LDA-NL levels, but not very much so. In particular, at the LDA-NL scheme the CNCN molecule binds 0.32 eV (7.4 kcal/mol) stronger than CO. This is due to a somewhat more favorable σ bond (ΔE_{A1}) and a clearly stronger π bond (ΔE_E), which together more than compensate the slightly more repulsive ΔE^0. The individual contributions to ΔE^0 exhibit larger differences, which demonstrates the generally occurring compensating effects of more positive Pauli repulsion and more negative electrostatic attraction when the metal−ligand bond becomes somewhat shorter, and when there are more occupied orbitals, as for CNCN as compared to CO. The σ bond (ΔE_{A1}) is only slightly stronger for CNCN, and indeed also the σ donation (depletion of 5σ and 9σ, respectively, and population of $10a_1$), is remarkably similar for CO and CNCN. As noted above, one expects the π bonding (ΔE_E) to be stronger in CNCN because of the relatively low position of the π-acceptor LUMO $3\pi^*$, and this effect does occur but it is rather moderate. Also, the π-backdonation (population of $2\pi^*$ and $3\pi^*$, respectively, depletion of 8e) is somewhat larger for CNCN, but not much. In this respect, it should be noted that in spite of the smaller Cr−C bond distance for the CNCN ligand, the π overlap (between the π acceptor on the ligand ($2\pi^*$ respectively $3\pi^*$) and the 8e π donor on $Cr(CO)_5$) is actually smaller for the CNCN than for the CO ligand. This can be rationalized by taking into account the fact that the $2p_\pi$ atomic orbital of the coordinating C has a larger contribution in the $2\pi^*$ orbital of CO (1.020) than in the $3\pi^*$ orbital of CNCN (0.831). The lower $3\pi^*$ energy makes the π bond nevertheless stronger, and accordingly, there is somewhat more π backdonation toward CNCN and somewhat stronger π (back)bonding.

In summary, one can conclude that the σ-base properties of CO and CNCN ligands are very similar but that the CNCN ligand is a somewhat stronger π-acid ligand. This was expected from the relative HOMO and LUMO energies of the CNCN and CO ligands, but we have noted that the effect remains moderate due to the smaller π overlap with the metal in the CNCN case.

(d) UV−vis Spectrum. The lowest singlet excitation energies present in the $Cr(CO)_5CNCN$ complex are given in Table 6. To visualize the energetic order of the highest occupied and lowest unoccupied orbitals, we give an orbital energy diagram in Figure 4 that contains, apart from the highest occupied "t_{2g}" derived levels, all

(35) (a) Hay, P. J. *J. Am. Chem. Soc.* **1978**, *100*, 2411. (b) Demuynck, J.; Kochanski, E.; Veillard, A. *J. Am. Chem. Soc.* **1979**, *101*, 3467.

Table 6. LDA, LDA-NL, and Experimental UV−Vis Spectral Data of $Cr(CO)_5CNCN$ in Dimethylbutane/Pentane (8:3)[a]

	LDA	LDA-NL	exp
$10e \rightarrow 11e$	3.79	3.51	3.68
$2b_2 \rightarrow 11e$	4.10	3.73	3.68
$10e \rightarrow 15a_1$	4.33	3.86	4.19
$2b_2 \rightarrow 15a_1$	4.35	4.00	4.19
$2b_2 \rightarrow 1\,2e$	4.57	4.19	4.64
$10e \rightarrow 12e$	4.64	4.33	4.64
$2b_2 \rightarrow 5b_1$	4.74	4.29	4.64
$10e \rightarrow 5b_1$	4.84	4.51	4.64
$10e \rightarrow 13e$	5.42	4.97	5.34
$2b_2 \rightarrow 13e$	5.48	5.14	5.34
$10e \rightarrow 3b_2$	5.52	5.05	5.34
$2b_2 \rightarrow 3b_2$	5.73	5.51	5.34

[a] Energies are given in electronvolts.

CO $2\pi^*$ derived levels, including the antibonding "t_{2g}*" counterparts of the occupied t_{2g} levels, as well as the CNCN $3\pi^*$ (the LUMO 11e) and the nominally 3d-e_g type levels $6b_1$ and $16a_1$, which contain a considerable amount of antibonding CO 5σ. The procedure used here for calculating multiplet energies and in particular singlet excitation energies was put forward by Ziegler *et al.*[27] These authors have argued that it is not possible to use the up- and down-spin densities of an arbitrary configuration state function, or of the average of configuration, in the currently used exchange-correlation functionals, since the effective exchange hole in these energy expressions may violate certain conditions that enter the derivation of the model functionals. These conditions are always met by single-determinant wave functions, and it is therefore recommended in ref 27 to resolve multiplet splittings by evaluating single-determinant energies with the exchange-correlation model functionals. This allows singlet−triplet splittings to be determined, and most of the spatial splittings. We restrict ourselves here to only calculating the singlet−triplet splittings; the terms of different spatial symmetry corresponding to an excited configuration are averaged since neither the theoretical accuracy nor the experimental resolution would warrant the spatial splittings to be calculated. Only the excitation energies to the singlet excited states corresponding to the specified configuration, averaged over the spatial multiplets where appropriate, are given in Table 6.

The experimental excitation energies represent rather broad bands in the UV−vis spectra, cf. Figure 1. The UV−vis experimental spectrum of the octahedral $Cr(CO)_6$ complex shows two bands at 4.44 and 5.48 eV[14f] corresponding to the transitions from the $2t_{2g}$ to the lowest unoccupied orbitals, the $6t_{2u}$ LUMO (mostly CO $2\pi^*$) and $2t_{1u}$ LUMO+1 (purely CO $2\pi^*$). These transition energies are calculated at 4.43 and 4.85 eV within the LDA scheme. Gray has assigned a weak shoulder at 335 nm (3.70 eV) to a LF transition, but we do not find such a low-lying LF transition in $Cr(CO)_6$. As a matter of fact, as in the $Cr(CO)_5CNCN$ complex (Figure 4), we find the e_g* levels in $Cr(CO)_6$ rather high up in the CO $2\pi^*$ spectrum of levels, even above the t_{2g}*. Therefore, we cannot assign the low-energy shoulder to the LF transition. Comparing these data to those of the $Cr(CO)_5CNCN$ complex, one may expect two features. First, the low-lying CNCN $3\pi^*$ is introduced into the virtual spectrum (11e), and we may expect low-energy transitions from "t_{2g}" ($2b_2$,10e) to this orbital. According to the calculations, such low-energy excitations do occur, and these transitions should fall under the extended low-intensity band at low energy (330−360 nm) in the experimental spectrum (the experimental band at 3.68 eV (337 nm) in Table 6). The intensity of this transition seems too low for assignment to an MLCT transition, but the calculations offer no alternative and the presence of this band in the experimental spectrum of $Cr(CO)_5CNCN$ and absence in $Cr(CO)_6$ is in agreement with this assignment. The second change expected in $Cr(CO)_5CNCN$ is that orbitals will split due to the symmetry lowering from O_h to C_{4v} and there will be a larger number of transitions (more excitations to fall under the experimental bands). However, due to the large similarity in the coordinative behavior of CNCN and CO, the splittings are usually not large. For instance, the HOMO $2t_{2g}$ orbital of $Cr(CO)_6$ is decomposed into the quite close-lying $2b_2$ (HOMO) and 10e orbitals of $Cr(CO)_5CNCN$ (Figure 4). As one can see from Table 6, these two orbitals lead to transitions of almost the same energy, which will reduce the total number of observed bands. It is difficult to make a definitive assignment. We can tentatively assume that the bands due to transitions to the 12e and $5b_1$ overlap, because of the small calculated difference in excitation energy, and similarly for the transitions to the 13e and $3b_2$. These transitions would then give rise to the 4.64 and 5.34 eV observed bands, respectively. Finally, the transitions to the $15a_1$ explain the experimental band at 4.19 eV. All transitions, except those to the 11e CNCN $3\pi^*$ orbital, are transitions from the metal to the $2\pi^*$ system of CO. Rather than putting too much emphasis on the individual assignments above, we note

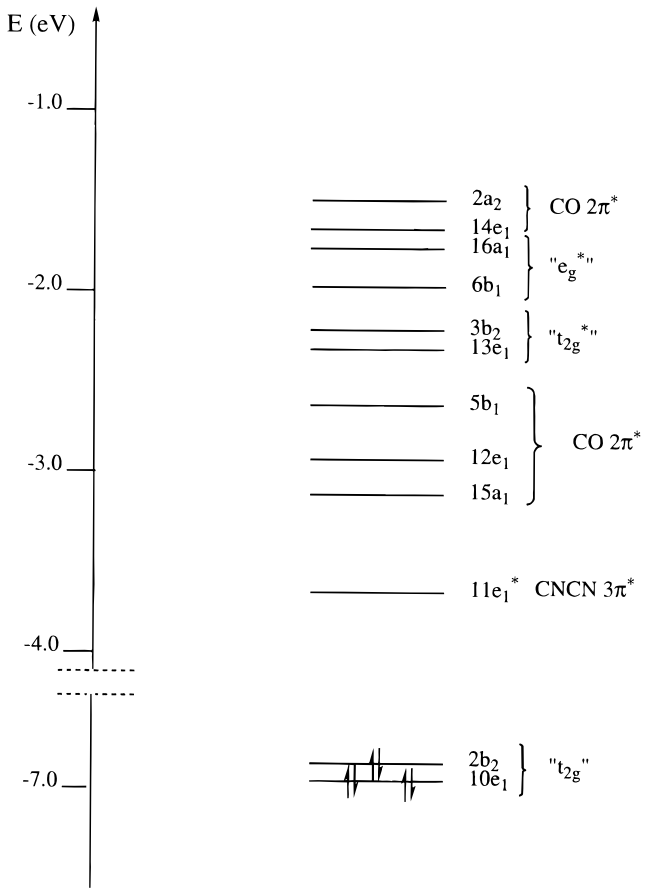

Figure 4. Orbital energy levels in the $Cr(CO)_5CNCN$ complex.

Table 7. Vertical LDA-NL Ionization Energies (from Unrestricted Kohn−Sham (UKS) Calculations on the Ions) and Experimental Photoelectron Spectra[a]

	LDA-NL/UKS	exp
10e	9.28	8.4
$2b_2$	9.39	8.4
9e	11.86	11.4−11.5
$14a_1$	12.73	>13
8e	13.29	>13
$13a_1$	13.26	>13

[a] Energies are given in electronvolts.

Table 8. LDA and Experimental Infrared Spectra of the $Cr(CO)_5CNCN$ Complex[a]

	type[b]	LDA	exp[c]	exp[d]
A_1	ν_s C≡NC≡N	2306	2246	2251
A_1	"A_{1g}"	2122	2102	2103
A_1	"E_g"(ν_{as} C≡NC≡N)	2051	2019	2020
B_1	"E_g"	2036		
A_1	"T_{1u}"	2032	1992	1993
E	"T_{1u}"	2015	1952	1951
				1962
				1925
a_1	CN−CN	1062		

[a] Spectra were measured in cyclohexane and frequencies are given in reciprocal centimeters. [b] The symmetries of the parent $Cr(CO)_6$ vibrational modes are given within quotes. [c] Reference 12. [d] Reference 13.

that the calculated excitation energies cover a range that agrees very well with the range of energies where the experimental spectrum exhibits absorption intensity.

(e) UV Photoelectron Spectrum. The values of the experimental and computed ionization energies (IEs) for the $Cr(CO)_5CNCN$ are gathered in Table 7. The experimental UV−PES spectrum of $Cr(CO)_5CNCN$ is shown in Figure 2. The geometry of the $Cr(CO)_5CNCN^+$ complex has been kept frozen at the LDA-NL $Cr(CO)_5$-CNCN-optimized geometry given in Table 3. All theoretical IEs have been computed within the spin-unrestricted formalism (unrestricted Kohn−Sham, UKS) including nonlocal corrections (LDA-NL/UKS).

There is reasonable agreement between the experimental and calculated IEs. This allows us to assign the experimentally observed bands. For instance, the 8.4 eV band corresponds to the 10e and $2b_2$ IEs. These orbitals have a large Cr 3d component. The calculated values for the IEs corresponding to the 10e and $2b_2$ orbitals are quite similar, in agreement with the presence of an only very slightly split band at 8.4 eV. However, we find ∼1.0 eV of discrepancy between the theoretical and experimental values. The 11.4−11.5 eV band can be assigned to the 9e orbital, which is basically the 2π orbital of CNCN. This agrees with this band occurring in the $Cr(CO)_5CNCN$ UV-photoelectron spectrum where there is a window in the $Cr(CO)_6$ spectrum between the 3d ionizations (also at 8.4 eV) and the band of CO $5\sigma/1\pi$ ionizations at 13.4 eV and higher. The same CO $5\sigma/1\pi$ band occurs in $Cr(CO)_5CNCN$, in agreement with the calculated ionization energies from the $14a_1$ orbital (5σ of CO), 8e orbital (1π of CO), and $13a_1$ orbital (8σ of CNCN). The calculated values, in particular from the $14a_1$ orbital, may be somewhat underestimated by our calculations.

(f) IR Spectrum. Table 8 contains the LDA harmonic theoretical frequencies together with the observed experimental frequencies (which are fundamentals, i.e., contain anharmonic contributions) for the $Cr(CO)_5CNCN$ complex in cyclohexane.

Since calculations of LDA-NL frequencies are computationally very demanding and given that it has been pointed out[32,36,37] that nonlocal corrections do not introduce important improvements in the calculated harmonic frequencies (see also Tables 1 and 2), at least when they are computed at the same reference geometry,[32] only LDA frequencies are reported in Table 8. The experimental frequencies are all lower than the calculated harmonic frequencies. As a matter of fact, it has been found[38] that the corrections to be applied to the fundamental frequencies so as to obtain the harmonic frequencies amount in the case of $Cr(CO)_6$ to values between +20 (A_{1g}, E_g) and +40 (T_{1u}) cm^{-1}. For the free CO molecule, the correction is also ∼+30 cm^{-1} (see Table 1). We note that applying a similar correction of 20−40 cm^{-1} to the corresponding experimental frequencies of $Cr(CO)_5CNCN$ (the $Cr(CO)_6$ "parentage" of the modes is indicated in Table 8) shows that the calculations agree very well with experiment. As a matter of fact, for $Cr(CO)_6$ we found with the present basis set very good agreement between calculated and experimental harmonic frequencies (for A_{1g}, E_g, and T_{1u}: 2139, 2043, and 2023 cm^{-1} calculated, 2139.2, 2045.2, and 2043.7 experimental[39]). A slightly larger difference, probably too large to be covered by anharmonicity corrections, is found for the highest A_1 mode in $Cr(CO)_5CNCN$, at 2310 cm^{-1}, which is basically the symmetric stretch mode of the CNCN triple bonds. Apart from anharmonicity effects, a further tendency to too-high calculated frequencies in these LDA calculations will arise from the too-short metal−ligand bond distances at the LDA level, as pointed out by Bérces and Ziegler.[32]

It is interesting to observe that CNCN distinguishes itself from CO in that there are two CNCN triple bond vibrations, the symmetric and asymmetric ones. The symmetric one has calculated frequency 2321 cm^{-1} (see Table 2) clearly distinct from the CO stretch of 2152 cm^{-1} (calculated), but the asymmetric CNCN triple bond vibration is calculated to be rather close (at 2082 cm^{-1}) to the CO stretch vibration (70 cm^{-1} difference; experimentally the difference between the fundamental frequencies, which are the only ones known for CNCN, is 10 cm^{-1} larger). The asymmetric CNCN triple bond vibration rather than the symmetric one is therefore expected to mix with CO vibrations in the complex. Indeed, we find in $Cr(CO)_5CNCN$ that the 2306 cm^{-1} harmonic frequency of symmetry A_1 can be assigned basically to the CNCN triple bond symmetric stretching mode, which shows very little mixing with the CO vibrations. Since this vibration was 2321 cm^{-1} (see Table 2) in the free CNCN ligand, the computed lowering for this frequency is only 15 cm^{-1}. The next A_1 harmonic frequency of 2122 cm^{-1} in the complex involves both CO stretch vibrations and the CNCN asymmetric stretch. In this mode, the CNCN vibrates "as the CO it replaces", as previously suggested on the basis of the experimental results.[13] As a matter of fact,

(36) Fan, L.; Ziegler, T. *J. Phys. Chem.* **1992**, *96*, 6937.
(37) Solà, M.; Mestres, J.; Carbó, R.; Duran, M. *J. Chem. Phys.* **1996**, *104*, 636.
(38) Jones, L. H.; McDowell, R. S.; Goldblatt, M. *Inorg. Chem.* **1969**, *8*, 2349.

the LDA harmonic frequency for the equivalent A_{1g} mode in $Cr(CO)_6$ is calculated to be 2139 cm^{-1}, i.e., only 17 cm^{-1} of difference. Since in the free CO the calculated stretch frequency is 2152 cm^{-1} (see Table 1), the harmonic frequency of this (still mostly CO) vibration is calculated to be lowered by 30 cm^{-1}. These frequency lowerings of 15 and 30 cm^{-1} assigned to CNCN and CO, respectively, within the limitations that should be clear from the above, are smaller than those deduced from experimental data. Actually, the observed lowering of the "CNCN symmetric stretching" is 51 cm^{-1} (2302−2251 cm^{-1}), whereas for the "CO stretching", the frequency is found to be lowered by 40 cm^{-1} (2143[1b]−2103 cm^{-1}). Most of the difference between the calculated lowering for the harmonic frequencies and observed lowering for the fundamentals can most likely (for CO certainly) be attributed to the too-low calculated harmonic frequencies of the free ligands; see section 2a. We return to the rather similar frequency lowerings for CNCN and for CO below.

The E_g mode in O_h $Cr(CO)_6$, which is computed at 2043 cm^{-1} at the LDA level, is split up in the A_1 and B_1 frequency modes with calculated frequencies 2051 and 2036 cm^{-1}. The 2036 cm^{-1} vibration is the B_1 equatorial CO stretching, which has zero intensity by symmetry. The CNCN triple bond asymmetric stretching vibration can only occur in the A_1 component, which in fact is again very much like the "A_1-type" of the degenerate set of E_g modes in $Cr(CO)_6$ with one axial CO stretch replaced by ν_{as} (CNCN). Note that the measured fundamental frequency (2020 cm^{-1}) is also very close to the E_g fundamental of $Cr(CO)_6$ (2026.7 cm^{-1}). The T_{1u} frequency of O_h $Cr(CO)_6$, which is 2023 cm^{-1} within the LDA approach, decomposes with very little shift into the closely spaced A_1 of 2032 cm^{-1} and the E of 2015 cm^{-1}. The observed fundamentals at 1993 and 1951 cm^{-1} are close to the T_{1u} fundamental of $Cr(CO)_6$ at 2000.4 and show a bit more spread and shift than the calculated harmonic frequencies.

The experimentally observed frequencies of 1962 and 1925 cm^{-1} were assigned to the $Cr(CO)_5NCNC$ complex in the experimental work.[13] We have not attempted to assign them here.

Finally, the A_1 mode of 1062 cm^{-1} corresponds to the CN−CN single bond stretching. This vibration is 975 cm^{-1} in the free ligand and it has *increased* as a result of the Cr 3d backdonation. As previously mentioned, the π backbonding of Cr to CNCN decreases the strength of the CN triple bonds and increases the CN−CN single bond strength. This fact is well reproduced by the LDA-computed harmonic frequencies.

Summarizing, we note that the substitution of one CO by CNCN distorts the IR spectrum remarkably little, both the calculated and the experimental spectra. This can be attributed to the presence of an asymmetric CNCN triple bond stretching mode that is close to the CO stretch and also couples to the CO vibrations very much like the stretch vibrations of the replaced CO would. These IR data indicate that electronically CNCN is similar to, and not a much better π acceptor, than CO. The similarity to CO is more striking than the difference. This gives support to our earlier finding that the relatively low position of the $3\pi^*$ LUMO of CNCN does not lead to much stronger π acceptor behavior.

Conclusions

The coordinative behavior of CNCN is found to be remarkably similar to that of CO, in spite of a clearly much lower lying π acceptor LUMO on CNCN (the C lone pair σ donor orbitals of CO and CNCN are very similar in spatial extent and energy). The low position of the $3\pi^*$ LUMO of CNCN does lead to calculated low-lying transitions in the $Cr(CO)_5CNCN$ UV−vis absorption spectrum, which are, however, only observed with very low intensity. Nevertheless, although the calculated first bond dissociation energy of CNCN is somewhat larger than for CO, the difference is modest. The low $3\pi^*$ does not lead to much stronger π-acceptor behavior of CNCN, as is also apparent from the very similar lowering of the CNCN stretch frequency compared to that of CO and to the fact that the CNCN stretch vibration (the asymmetric one) couples to the other CO stretches very much like the CO stretch it replaces. We have also observed in the decomposition of the bond energy that the σ and π components of the bond to the metal fragment are similar for CNCN and CO, the π bond being only some 20% stronger in the case of CNCN. The analysis of the bonding shows that the low position of the $3\pi^*$ is counteracted by a smaller overlap (hence smaller interaction matrix element) with the π-donor orbital of the metal fragment, due to the less pronounced C p_π character of the CNCN $3\pi^*$ LUMO than the CO $2\pi^*$ LUMO.

Acknowledgment. M.S. thanks the Direcció General de Recerca de la Generalitat de Catalunya for financial support through Contract EE93/1-122. E.J.B. thanks the Iberdrola foundation (Spain) for financial support and Prof. J. Bertrán for hospitality at the Universitat Autónoma de Barcelona.

OM960921B